Journal of Histochemistry & Cytochemistry 2017, Vol. 65(3) 153–171

DOI: 10.1369/0022155416686934
journals.sagepub.com/home/jhc
SAGE

Evaluation of Long-Term Cryostorage of Brain Tissue Sections for Quantitative Histochemistry

Larissa I. Estrada, Amy A. Robinson, Ana C. Amaral, Eustathia L. Giannaris, Nadine C. Heyworth, Farzad Mortazavi, Laura B. Ngwenya, Debra E. Roberts, Howard J. Cabral, Ronald J. Killiany, and Douglas L. Rosene

Department of Pharmacology and Experimental Therapeutics (LIE, AAR) and Department of Anatomy and Neurobiology (ACA, ELG, NCH, FM, LBN, DER, RJK, DLR), Boston University School of Medicine, Boston, Massachusetts, and Department of Biostatistics, Boston University School of Public Health, Boston, Massachusetts (HJC)

Summary

Storage of tissue sections for long periods allows multiple samples, acquired over months or years, to be processed together, in the same reagents, for quantitative histochemical studies. Protocols for freezer storage of free-floating frozen sections using sucrose with different additives have been reported and assert that storage has no effect on histochemistry, but no quantitative support has been provided. The present study analyzed the efficacy of long-term storage of brain tissue sections at −80C in buffered 15% glycerol. To determine whether histochemical reactivity is affected, we analyzed 11 datasets from 80 monkey brains that had sections stored for up to 10 years. For processing, sections from multiple cases were removed from storage, thawed, and batch-processed at the same time for different histochemical measures, including IHC for neuronal nuclear antigen, parvalbumin, orexin-A, doublecortin, bromodeoxyuridine, the pro-form of brain-derived neurotrophic factor, and damaged myelin basic protein as well as a histochemical assay for hyaluronic acid. Results were quantified using stereology, optical densitometry, fluorescence intensity, or percent area stained. Multiple regression analyses controlling for age and sex demonstrated the general stability of these antigens for up to a decade when stored in 15% glycerol at −80C. (J Histochem Cytochem 65:153–171, 2017)

Keywords

batch-processing, brain tissue, cryopreservation, cryoprotection, frozen sections, immunohistochemistry, stereology, quantification

Introduction

Histochemistry uses a variety of methods to localize substances in tissue sections, ranging from small peptides to large enzymes, as well as a variety of other substances. Although localization and colocalization on a qualitative level are often the initial interest, subsequent studies almost always require quantitative assessment of the amount and/or distribution of the histochemical target. The focus is often to quantify its presence, absence, or relative difference between regions and/or conditions. This is especially true in studies of the brain where histochemical assessments may occur across development, across aging, across species, across brain regions, or between different pathological or experimental states. For these quantitative comparisons, the

Received for publication September 19, 2016; accepted December 5, 2016.

Corresponding Author:
Larissa I. Estrada, Department of Pharmacology and Experimental Therapeutics, Boston University School of Medicine, 700 Albany St., W701, Boston, MA 02118, USA.
E-mail: larissa@bu.edu

ideal controlled experiment requires that the tissue sections to be analyzed should be processed together, under the same conditions and in the same reagents. Such designs are most feasible in small short-lived animals such as mice, where groups of control and experimental subjects (transgenic, aged, drug injected, etc.) can, with reasonable effort, be processed simultaneously. Such a design is not feasible if the tissue samples cannot be acquired at the same time. For example, in a study of the effects of age on neuron number in the visual cortex of the rhesus monkey,[1] 26 monkeys ranging in age from 7.4 to 31 years of age were behaviorally tested, and tissue was collected over a period of 8 years. Although frozen tissue sections were cut relatively soon after tissue collection, histochemical processing of individual cases over years would have introduced many uncontrolled between-subject factors. Similar constraints are present for human brain tissue acquired over years as well as for samples from other species where sample sizes are limited.

A potential solution to this problem was proposed by Watson and colleagues[2] who suggested storing cut tissue sections at –20C in a cryoprotectant developed by de Olmos and colleagues.[3] This cryoprotectant consists of a 30% sucrose solution in PBS with the "antifreeze" additives ethylene glycol (30%) and polyvinylpyrrolidone-40 (PVP-40; 1%). Tissue in this cryoprotectant can then, at some later time, be thawed and processed together. Other sucrose and ethylene glycol formulations omit the 1% PVP-40[4] or use phosphate buffer (PB) instead of PBS.[5] As a simpler alternative that avoids the dehydrating and shrinkage of 30% sucrose, we developed a protocol for cryostorage of sections at –80C in 0.1-M PB with 15% glycerol and no sucrose or other additives based in part on our success with a glycerol cryoprotection protocol for freezing large blocks of brain tissue without shrinkage or freezing artifact. This protocol incubates fixed tissue blocks in 0.1-M PB with first 10% glycerol and then 20% glycerol before flash freezing the block at –75C and then storing the block at –80C until it is cut into frozen sections.[6] This glycerol cryoprotection regimen is superior to sucrose for avoiding ice crystal artifact, especially for very large (≥100 cc) blocks of monkey or even human brain, and because it completely avoids the shrinkage and spatial distortion of brain tissue caused by dehydration during sucrose infiltration. Once cut, the sections are then transferred to the 15% glycerol cryoprotectant and stored at –80C until processed. Initial comparisons between tissue stored for many months in 15% glycerol at –80C with freshly cut tissue showed effective morphological preservation, so we have continued using this cryostorage regimen for more than a decade. Here, we have extracted the quantitative data from our prior studies of the effects of subject age on 11 different histochemical markers. These histochemical datasets were statistically analyzed using multiple regression to control for the original variables of interest, specifically age and sex, while assessing the effect of time stored at –80C on a variety of quantitative histochemical measures.

Materials and Methods

Subjects

Results reported are from 80 rhesus monkeys, 47 males and 33 females, that ranged in age from young (3 years) to the very old (31 years). This range corresponds to humans from 9 to about 90 years of age.[7,8] All monkeys were part of long-term studies of normal cognitive aging and were obtained from national primate centers after screening health records to verify known dates of birth and to exclude monkeys with histories that could confound investigations of brain aging. Different cohorts of animals and different samples sizes (n=16 to n=36) were drawn from this group and used for each of the different studies analyzed here. Details of this subject pool are summarized in Table 1. All procedures conformed to the National Institutes of Health (NIH) *Guide for the Care and Use of Laboratory Animals*[9] and were approved by the Institutional Animal Care and Use Committee of the Boston University Medical Campus.

Tissue Collection and Processing

Monkeys were deeply anesthetized and euthanized by exsanguination during transcardial perfusion fixation of the brain, either with ice-cold Krebs–Henseleit buffer followed by 4% paraformaldehyde in 0.1-M PB at pH 7.4 and 37C, or with just 4% paraformaldehyde without the Krebs first (Table 2). Four monkeys (AM143, AM133, AM144, and AM209) were instead perfused with 1% paraformaldehyde and 1.25% glutaraldehyde in 0.1-M PB. Differences in fixation type were not found to affect staining. Brains were blocked in situ in the coronal plane, removed intact, weighed, photographed, and postfixed for less than 24 hr.[1,10] They were then cryoprotected by immersion in 10% glycerol and 2% DMSO in 0.1-M PB until the block sank, indicating equilibration between the block and the solution (1–3 days depending on block size), and then transferred to PB with 20% glycerol and 2% DMSO until equilibrated, as indicated by sinking (3–5 days). Blocks were then flash frozen in –75C isopentane and placed into storage at –80C until they could be cut into frozen sections.[6]

Table 1. Subjects.

Histochemical Staining Measure	Number of Subjects	Males	Females	TTF Range
NeuN cell #	26	11	15	0.04–8.25
PV cell #	26	11	15	1.82–10.03
Orexin-A cell #	36	18	18	0.15–6.81
BrdU cell #	16	16	0	0.32–3.79
DCX cell #	16	16	0	0.32–3.79
proBDNF^{+} cell #	36	19	17	0.43–7.65
proBDNF^{+} puncta #	36	19	17	0.43–7.65
proBDNF OD in GM	36	19	17	0.43–7.65
proBDNF OD in WM	36	19	17	0.43–7.65
dMBP fluorescence intensity	29	13	16	1.15–10.89
HA percent area	29	13	16	1.15–10.89

The number of subjects and range of freezing times (TTF) are shown for each cohort. Some staining measures were acquired as double labels and, thus, share a cohort and/or TTF range. These include NeuN and PV (same cohort, separate experiments), BrdU and DCX (same cohort, separate experiments), dMBP and HA (double label; same cohort and TTF range), and all proBDNF stains (different analysis measures derived from one batch of immunostained tissue). Abbreviations: TTF, total time frozen; NeuN, neuronal nuclei; PV, parvalbumin; BrdU, bromodeoxyuridine; DCX, doublecortin; proBDNF, pro-brain-derived neurotrophic factor; OD, optical density; GM, gray matter; WM, white matter; dMBP, damaged myelin basic protein; HA, hyaluronic acid.

Table 2. Timeline of Tissue Processing.

Step	Procedure	Solution	Duration
1	Subject perfused	4% paraformaldehyde or Krebs buffer, and then 4% paraformaldehyde (two-stage perfusion)	
2	Brain postfixed	4% paraformaldehyde	24 hr
3	Cryoprotection stage 1	10% glycerol + 2% DMSO	1–3 days
4	Cryoprotection stage 2	20% glycerol + 2% DMSO	3–5 days
5	Flash freeze the cryoprotected block and hold at −75C for 1 hr	−75C isopentane	Begins "total time frozen"
6	Move frozen block to −80C storage		Until next step (days to years)
7	Cut frozen block cut on freezing sliding microtome and rapidly thaw sections on blade	Collect thawed tissue sections in 15% glycerol	Store at 4C overnight
8	Freeze sections at −80C	Same 15% glycerol	Until next step (days to years)
9	Thaw all sections rapidly as needed for batch-processed histochemical study		Ends "total time frozen"

The steps used to obtain, cryoprotect, cut into sections, and store tissue sections before histochemical processing are shown in order. The total time frozen encompasses the time between flash freezing the cryoprotected block (step #5) and thawing tissue sections on the first day of histochemical processing (step #9). All solutions are prepared in 0.1-M phosphate buffer, pH 7.4.

For cutting, the frozen blocks were removed from –80C storage, affixed to a freezing stage of a sliding microtome, and maintained frozen by being surrounded with pulverized dry ice that was repacked every 15 to 20 min. Blocks were cut into 10 interrupted series of 30-µm-thick frozen sections. As they were collected, the sections in a series were distributed across 24 vials (polystyrene hematology cell counter vials, #9040; USA Scientific, Ocala, FL), with each vial containing about six to eight sections in 15 to 20 ml of 15% glycerol in PB. Sections were allowed to equilibrate in the 15% glycerol overnight at 4C and were then refrozen by transferring the vials into a –80C freezer, where they were kept until thawed for processing.

Tissue for each study was "batch-processed" by removing the appropriate vials from the –80C freezer, at the same time, for all the cases selected for that study. Sections were immediately thawed by placing the vials in a room temperature water bath for about 30 min. Sections were then processed together in the same reagents. The number of sections per subject varied according to the design of the aging study for which they were originally prepared, and was chosen to yield an appropriate sample size based on the size

Table 3. Antigens Studied in Batch-Processed Datasets.

Dataset	Antigen	Antibody	Company
NeuN (clone A60)	Soluble nuclear protein in neurons, 46-kDa and 48-kDa isoforms	Mouse monoclonal	MAB377, lot LV1388597; Chemicon, Temecula, CA
PV	Calcium-binding protein found in GABAergic interneurons	Mouse monoclonal	PV235; Swant, Marly, Switzerland
Orexin-A (C-19)	Excitatory neuropeptide hormone	Goat polyclonal	SC-8070; Santa Cruz Biotechnology, Dallas, TX
BrdU	Synthetic analogue of thymidine; nuclear localization	Mouse monoclonal	Chemicon
dMBP	Amino acids 69 to 86 of guinea pig myelin basic protein	Rabbit polyclonal	AB5864, lot 2382586; Millipore, Billerica, MA
DCX	Microtubule-associated protein	Rabbit polyclonal	#4604; Cell Signaling Technology, Danvers, MA
HA	HA, the major glycosaminoglycan component of neural extracellular matrix	NA (cow-derived HA-binding protein)	#385911, lot D00155144; Millipore
proBDNF	Precursor of BDNF, a member of the neurotrophin family of growth receptors	Rabbit polyclonal	ANT-006, lot AN-05; Alomone Labs, Jerusalem, Israel

Abbreviations: NeuN, neuronal nuclei; PV, parvalbumin; GABA, gamma-aminobutyric acid; BrdU, bromodeoxyuridine; dMBP, damaged myelin basic protein; DCX, doublecortin; HA, hyaluronic acid; proBDNF, pro-brain-derived neurotrophic factor.

of the region of interest and the frequency of the cell or structure to be analyzed. The number of sections analyzed per subject for each study is as follows: hyaluronic acid (HA)/damaged myelin basic protein (dMBP) = 6 to 8, neuronal nuclei (NeuN)/parvalbumin (PV) = 6 to 8, orexin-A = 14, bromodeoxyuridine (BrdU)/doublecortin (DCX) = every 20th section through the entire hippocampus, and pro-brain-derived neurotrophic factor (proBDNF) = 20 to 22. The details that apply to all the studies have been published[1,10] but are summarized below for those yet to be published.

IHC

The antigens studied are listed in Table 3, and examples of staining are shown in Fig. 1. All IHC protocols included a variation of the following basic steps: After thawing, free-floating sections were rinsed 3 to 6 times for 5 min each in buffer (e.g., PB) to remove glycerol. This was often followed by quenching of endogenous peroxidases in 1% to 3% hydrogen peroxide, treatment in blocking serum to reduce binding at nonspecific sites, incubation in primary antibody, and incubation in secondary antibody. Buffer washes (potassium phosphate–buffered saline [KPBS], PBS, PB, or TBS, pH 6.8–7.4) were interposed between all basic steps.

For fluorescent staining, an Alexa-labeled secondary antibody was used. Following incubation with the Alexa secondary antibody, tissue was mounted onto gelatin-subbed glass slides, treated with an autofluorescence elimination reagent (Millipore's autofluorescence eliminator reagent, #2160, and accompanying instructions), coverslipped with antifade polyvinyl alcohol mounting medium (Sigma, St. Louis, MO), and stored in the dark at 4C.

For chromogen-labeled tissue, incubation with a biotinylated secondary antibody was followed by avidin–biotin amplification using a VECTASTAIN ABC Elite kit (Vector Laboratories), and chromogen development. Once the reaction was complete, sections processed for chromogenic visualization were mounted on gelatin-subbed slides, dried overnight, dehydrated in graded alcohols, cleared in xylene, and coverslipped.

Additional steps for some protocols included postfixation of sections in 2.5% acrolein and 4% paraformaldehyde in potassium PBS (proBDNF staining protocol[11]); antigen retrieval with formamide, heat, or acid (BrdU and DCX protocols[10,12]); quenching in 3% hydrogen peroxide in methanol instead of buffer (proBDNF staining protocol); a Nissl counterstain[1]; or processing in a PELCO BioWave Pro 36500 laboratory microwave system (HA and dMBP staining protocol).

HA Histochemistry

HA histochemistry was performed using biotinylated HA-binding protein (bHABP) as the probe, a technique developed by Ripellino and colleagues.[13] Because this differs from the IHC procedures of the other markers but was run as a double-label experiment with IHC, the relevant details are as follows: Sections were thawed and

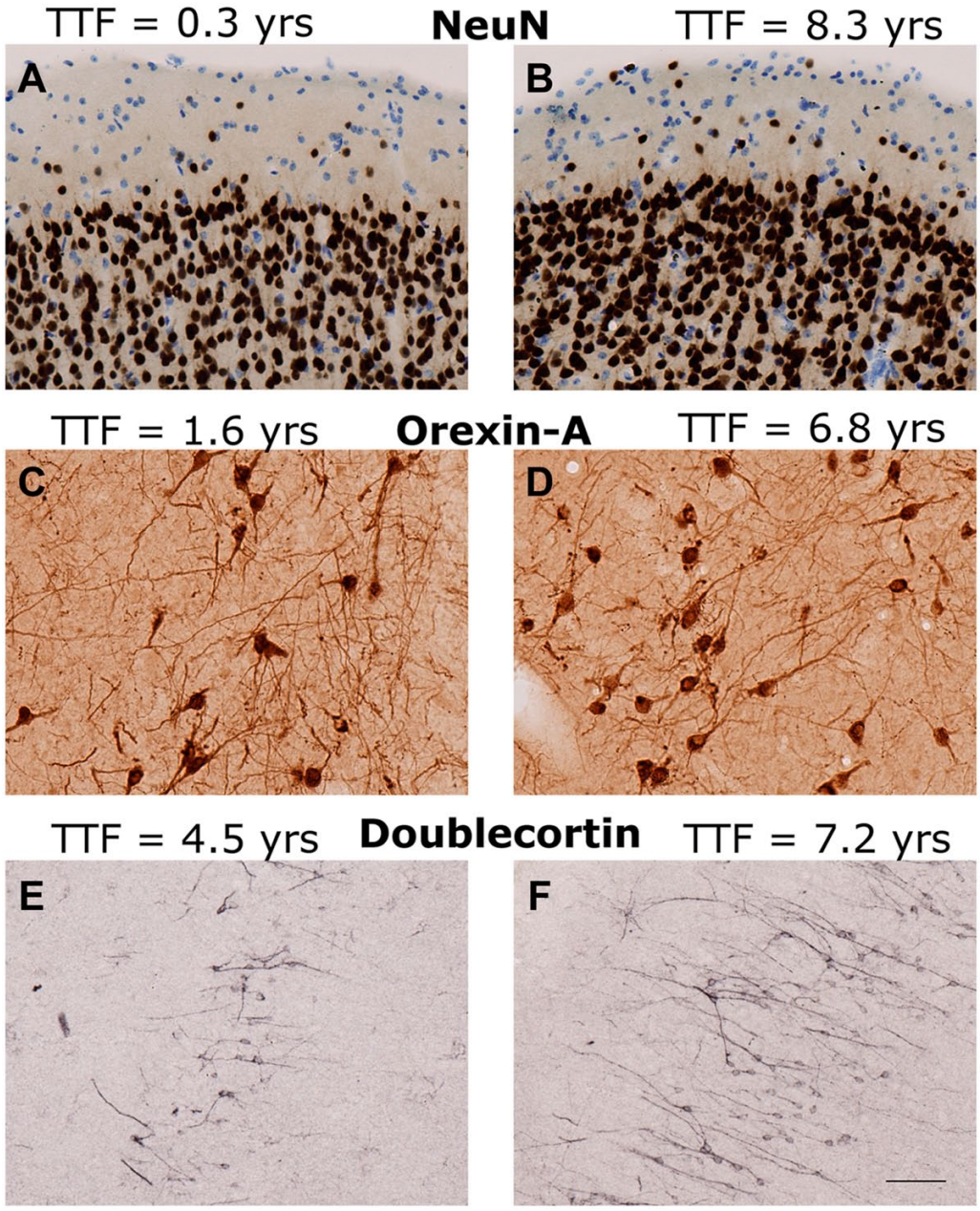

Figure 1. Examples of immunohistochemical staining. Examples of IHC staining in age- and region-matched sections with short (left A, C, E) and long (right B, D, F) cryostorage times (TTF). (A, B) NeuN in area 17 of visual cortex of (A) AM242, a 23.5-year-old male, and (B) AM104, a 28.9-year-old female. (C, D) Orexin-A in hypothalamus of (C) AM189, a 24.4-year-old male, and (D) AM064, a 24.9-year-old male. (E, F) Doublecortin in the dentate gyrus of (E) AM247, a 6.9-year-old male, and (F) AM132, a 7.5-year-old male. Abbreviations: TTF, total time frozen; NeuN, neuronal nuclei. Scale bar = 50 µm.

rinsed with KPBS (pH 7.3) between each step. They were then incubated in blocking serum for 1 hr and then in a KPBS–triton solution containing 1:500 bHABP (Millipore) and 1:750 anti-dMBP antibody (Millipore). This incubation step began in a microwave (PELCO BioWave Pro 36500 laboratory microwave system) set at 250 W and 20 mm Hg vacuum for 6 min, and then continued for 18 hr on a rocker at 4C. Next, the sections were incubated in a KPBS–triton solution containing secondary antibodies (streptavidin-conjugated Alexa 488 to label the bHABP and 1:500 goat anti-rabbit IgG Alexa 568; Invitrogen, Carlsbad, CA) in the microwave

set at 250 W without vacuum for 6 min, followed by 2 hr at room temperature. Sections were then rinsed, mounted onto gelatin-subbed slides, treated with autofluorescence eliminator reagent (Millipore) according to manufacturer instructions, and then coverslipped with polyvinyl alcohol mounting medium (Sigma #10981). Coverslipped slides were stored in the dark, allowed to dry at room temperature for 48 hr, and then were sealed with nail polish and stored in the dark at 4C.

Quantification With Stereology

For quantification with stereology, an expert observer used the Stereo Investigator (MicroBrightField Inc., Williston, VT) or BIOQUANT Stereology Toolkit (BIOQUANT Inc., Nashville, TN) systems to mark and count the cells positive for a particular label using the optical fractionator method of West and colleagues.[14] Detailed representative descriptions can be found for NeuN in Giannaris and Rosene[1] and for BrdU in Ngwenya et al.[10] This approach obtains an estimate of the total number of labeled objects in a defined region of interest.

Quantification of Digitized Images With ImageJ

Alternatively, sections were digitized at an appropriate power (e.g., 20× for HA and dMBP) using a Nikon E600 Microscope (Nikon, Tokyo, Japan) equipped with a motorized stage and controlled by either Turboscan montaging system software (Objective Imaging Ltd., Cambridge, UK) or Stereo Investigator software (MicroBrightField Inc.). The images were then quantified using ImageJ. Details of this approach for measures reported here but not yet published are given in the following sections.

ProBDNF

After processing with IHC for proBDNF, tissue sections were digitized and the images analyzed to obtain counts of positively stained cell bodies (neurons and glia), counts of puncta (staining in axons, dendrites, and glial processes), and measurements of the overall optical density (OD) of staining in gray matter and in white matter. To obtain digitized images, a systematic random sample was acquired at 100× using Stereo Investigator software (v9.14.3). ImageJ (v1.45s[15]; NIH, http://imagej.nih.gov/ij) was then used to enhance the image contrast, apply a threshold to distinguish positively stained features from the background, and apply a size exclusion threshold to identify and distinguish somata and puncta. For the analysis of the OD of proBDNF, photomontages through the entire region of interest were obtained using Turboscan software (Surveyor v6.1.0.3; Objective Imaging Ltd.) with a Nikon 20× Plan Fluor objective at a constant exposure time for all images. To measure the OD of the sections, ImageJ was first used to outline the regions of interest. Then, the uncalibrated OD function of ImageJ was used to transform the mean gray value of each pixel to OD according to the formula, Uncalibrated OD = $\log_{10}$(255/pixel value).

HA and dMBP

For epifluorescent digitization, optimal exposure time was determined for each label using test tissue that was processed in the same batch as the sections for the full analysis to avoid potentially fading the study sections. Each region of interest was then digitized twice—once using the excitation wavelength and optimal exposure time for one fluorophore, and then under the optimal conditions for the other. The order in which subjects were digitized was counterbalanced across age and sex. ImageJ was used to select anatomically defined samples from regions of interest within photomontages, apply thresholds, and either obtain the percent area stained or calculate a measure of fluorescence intensity. The intensity measure used is analogous to methods used by Yamamoto et al.[16] and Ihara et al.[17]

Total Time Frozen (TTF)

The tissue processing protocol is described in section "Materials and Methods" and shown in Table 2. The measure of freezing time analyzed in this study, TTF, encompasses the period of time starting when a cryoprotected tissue block is frozen in –75C isopentane, and ending the day vials containing tissue sections cut from that block were thawed for processing. There is one freeze–thaw cycle within this TTF period, occurring when the block is sectioned, but sections thaw rapidly onto the knife as they are cut and remain thawed as they equilibrate in the 15% glycerol buffer for less than 24 hr. They are then refrozen to –80C in an ultralow freezer. It is worth noting that TTF is a composite of the time stored as a cryoprotected block before cutting plus the time stored as sections in 15% glycerol at –80C. These component measures were analyzed along with TTF, but as the results exactly paralleled those of TTF, only the TTF analyses are shown here.

Data Analysis and Statistics

The primary aim of this study was to determine whether time frozen at –80C affects quantitative histochemistry. The histochemical measures for each of 11

datasets (e.g., NeuN cell counts, or HA percent area, etc.) were treated as the dependent variables in all analyses. As the staining measures were produced from several different studies, and each study used a distinct subject cohort with only minimal overlap and was performed on a different date, each staining measure, even for cases used in multiple studies, had different data for its associated "TTF" variable.

Multiple regression analyses were performed using Statistical Analysis Software (SAS; v9.3), and summary statistics are reported in Table 4. The linearity assumption was assessed by testing the significance of squared TTF terms. If TTF^2 was a significant predictor of the dependent histochemical variable, a nonlinear model (quadratic) was used instead of a linear model. Interaction variables were tested to detect the presence of combined effects of two predictors. For example, testing the significance of an age–TTF interaction variable (created by multiplying age times TTF for each subject) in a multiple regression model would enable the detection of "confounding" effects that would be present if tissue from young monkeys had significantly different TTF values than tissue from aged monkeys. If the young monkeys in a particular study were frozen for a significantly longer (or shorter) period of time than the aged monkeys, the interaction between age and TTF would be significant. All interaction variables of interest were tested for all datasets, and the only one that reached significance was the relationship between subject age and TTF for the orexin dataset (p=0.032; Table 4). However, as there was no correlation between TTF and orexin, the potential effect of the age–TTF interaction for orexin does not affect the outcome of any tests relevant to this study.

The multiple regression analyses were performed using a stepwise approach. In other words, each histochemical measure (dependent variable) was modeled using several predictors of interest (independent variables), including sex, age, TTF, and relevant interaction variables. The SAS regression output includes the p value of each predictor in the model. When there were predictors with p values greater than the alpha cutoff (0.05 in this study), the predictor with the least significant (i.e., greatest) p value was eliminated from the model, and the regression was run again. This one-by-one elimination of the least significant predictor continued until only significant predictors remained. The model that included only significant predictors at $\alpha = 0.05$ was considered the best model.

Because age and sex are variables of interest in many of the studies for which these datasets were prepared, Table 4 lists the summary statistics of regression models that include age and sex even if they did not reach significance. This information is useful for assessing the relative contribution of each predictor to the overall model (e.g., for comparing whether TTF or age accounts for more of the variance of a particular staining measure). Summary statistics for the best model are reported in section "Results" for each staining measure.

Explanation of Output Statistics in Multiple Regression

Table 4 lists five statistics: (1) the β estimate, (2) the standardized β estimate, (3) the p value, (4) the semipartial R^2, and (5) the overall model R^2.

1. The β estimate is interpreted as the amount of change in the dependent variable for a one-unit increase in the independent variable. In Table 4, the β estimate is reported with a 95% confidence interval.
2. The standardized β estimate is derived by converting the β estimate into standard deviation units. This statistic is, thus, interpreted as the amount of change in the dependent variable for a one standard deviation change in the independent variable. While the non-standardized β estimates for variables within a model may have different units from one another (because each has the same units as the variable it describes), the standardized β estimates are all on the same scale. Standardized β estimates from different variables within the same model can, thus, be directly compared to determine which has a greater effect on the dependent variable.
3. The p value is the probability of finding a result as extreme or more extreme than what was observed given that the null hypothesis is true. The p value is used to assess the significance of these statistical tests by comparing the p value probability with a predetermined "alpha" threshold. The alpha threshold chosen for this study was 0.05, so if the p value was less than 0.05, the null hypothesis is rejected.
4. The semipartial R^2 is a measure of how much each individual independent variable contributes to the R^2 of the overall model, which is the proportion of variance accounted for by that variable.
5. The overall model R^2 can be interpreted as the proportion of the variability of the dependent variable that is accounted for by all the predictors in the model.

Table 4. Summary of Regression Statistics for Models in Which TTF Is a Significant Predictor.

Staining Measure (Dependent Variable)	Independent Variable	*p* Value	β Estimate (95% CI for Significant Predictors)	β Estimate (Standard Units)	Semipartial R^2
Orexin-A	TTF	0.087	−7.188 (−15.488, 1.111)	−0.885	0.072
	TTF × Age	0.032	0.442 (0.041, 0.843)	1.357	0.116
	Age	0.002	−537.209 (−857.666, −216.752)	−0.924	0.269
	Sex	0.452	−970.000	−0.117	0.133
				Model R^2=	0.288
PV	TTF	0.045	−10,578 (−20,871, −284.110)	−1.876	0.173
	TTF^2	0.054	2.597 (−0.050, 5.244)	1.805	0.157
	Age	0.723	55,376	0.074	0.005
	Sex	0.992	−19,760	−0.002	<0.001
				Model R^2=	0.206
DCX	TTF	0.086	−3.610 (−7.802, 0.582)	−0.340	0.104
	Age	0.006	−346.482 (−573.541, −119.423)	−0.603	0.325
	Sex		NA	NA	NA
				Model R^2=	0.611
proBDNF somata	TTF	0.008	6.27×10^{-6} (1.79×10^{-6}, 1.08×10^{-5})	0.408	0.165
	Age	0.004	8.96×10^{-4} (3.11×10^{-4}, 1.48×10^{-3})	0.449	0.197
	Sex	0.618	−0.002	−0.072	0.005
				Model R^2=	0.352
proBDNF WM OD	TTF	0.031	1.66×10^{-5} (1.59×10^{-6}, 3.15×10^{-5})	0.357	0.126
	Age	0.065	1.83×10^{-3} (-1.23×10^{-4}, 3.79×10^{-3})	0.304	0.091
	Sex	0.861	−0.002	−0.028	0.001
				Model R^2=	0.205
dMBP fluorescence intensity	TTF	0.081	-9.20×10^{-3} (-1.96×10^{-2}, 1.24×10^{-3})	−1.935	0.082
	TTF^2	0.036	2.36×10^{-6} (1.71×10^{-7}, 4.55×10^{-6})	2.388	0.123
	Age	0.120	0.180	0.260	0.064
	Sex	0.046	3.757 (0.074, 7.440)	0.356	0.110
				Model R^2=	0.405
HA percent area	TTF	0.011	−0.010 (−0.018, −0.003)	−2.564	0.144
	TTF^2	0.003	2.58×10^{-6} (9.55×10^{-7}, 4.20×10^{-6})	3.067	0.203
	Age	0.031	0.191 (0.019, 0.362)	0.323	0.099
	Sex	0.113	2.116	0.236	0.048
				Model R^2=	0.548

The 95% CI is shown only for the β estimates of predictors that approach or attain significance. "Model R^2" is the unadjusted R^2 for the model that includes the variables shown. See section "Materials and Methods" for further explanation of these statistical measures. Abbreviations: TTF, total time frozen; CI, confidence interval; PV, parvalbumin; DCX, doublecortin; proBDNF, pro-brain-derived neurotrophic factor; WM, white matter; OD, optical density; dMBP, damaged myelin basic protein; HA, hyaluronic acid.

Results

NeuN Cell Counts

NeuN is an immunohistochemical marker for neurons where it mainly labels nuclei.[18] It is now known that NeuN is the Fox-3 splicing factor.[19] Stereological counts of $NeuN^+$ neurons in primary visual cortex of the aging monkey brain showed no effect of age (p=0.929, R^2 < 0.001) as previously reported.[1] As shown in Fig. 2A, there was no association between TTF and NeuN counts (p=0.795, R^2 = 0.003). There was also no relationship between TTF and NeuN counts in a multiple regression analysis controlling for age and sex (TTF p=0.723, semipartial R^2 = 0.006).

Orexin-A Cell Counts

Orexin-A, also known as hypocretin 1, is an excitatory neuropeptide hormone.[20] Stereological counts of orexin-A-positive neurons in the hypothalamus of the aging monkey brain showed a significant negative relationship of age in males but not females (p=0.026, R^2 = 0.138). In the multiple regression analysis that tested for interactions between TTF, age, and sex,

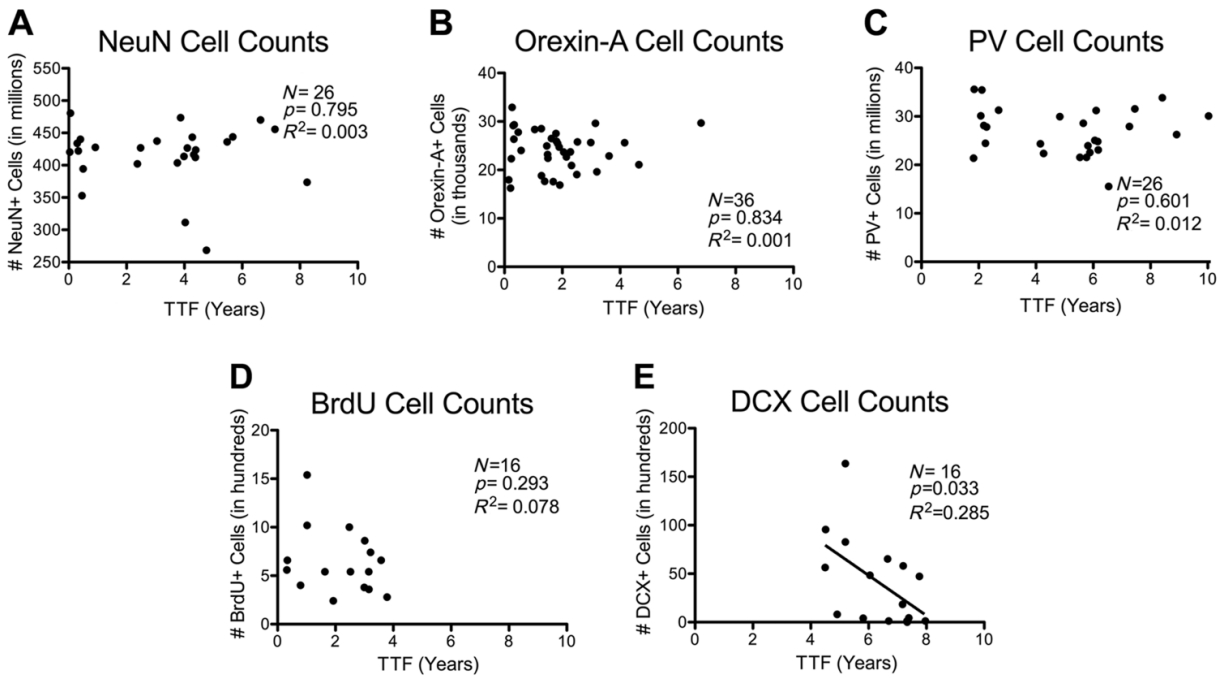

Figure 2. Simple linear correlations between TTF and stereological cell counts. TTF in years versus stereological counts for the following antigens: (A) NeuN, a marker of neurons, counted in cortical area 17; (B) orexin-A, an excitatory neuropeptide hormone produced by a subpopulation of neurons, counted in hypothalamus; (C) parvalbumin, a calcium-binding protein used to label a subpopulation of GABAergic interneurons, counted in cortical area 17; (D) BrdU, a marker of newly generated cells, counted in dentate gyrus; (E) DCX, a marker of immature neurons and neuronal precursors, counted in dentate gyrus. Abbreviations: TTF, total time frozen; NeuN, neuronal nuclei; GABA, gamma-aminobutyric acid; BrdU, bromodeoxyuridine; DCX, doublecortin; PV, parvalbumin; DCX, doublecortin.

there was a significant interaction between TTF and age (p=0.032) reflecting a positive correlation between TTF and age (r = 0.317). Thus, for this cohort, tissue from aged monkeys was stored in the freezer longer than tissue from young monkeys. Nevertheless, the correlation between TTF and orexin cell count was not significant in any of three models considered: (1) a single linear regression (p=0.834, R^2 = 0.001; Fig. 2B); (2) a multiple regression model that included the TTF–age interaction variable, TTF, age, and sex (TTF p=0.087, semipartial R^2 = 0.072; Table 4); or (3) a multiple regression model that contained only the TTF–age interaction variable, TTF, and age (same as #2 but excluded sex due to its non-significant p value). In this third model, TTF p=0.103 and semipartial R^2 = 0.064.

PV Cell Counts

PV is a calcium-binding protein that is used as a marker of subpopulations of GABAergic (gamma-aminobutyric acid) interneurons.[21] Stereological counts of PV^+ neurons in primary visual cortex of the aging monkey brain showed no effect of age (p=0.404, R^2 = 0.029).[1] When analyzed for effects of cryostorage, a single linear regression between only TTF and PV is not significant, with p=0.601 and R^2 = 0.012 (Fig. 2C). The relationship between TTF and PV was more accurately fit by a quadratic multiple regression model than by a simple linear model. The quadratic multiple regression model that contained only TTF^2 and TTF as independent variables was best, and approaches significance (overall model p=0.075, R^2 = 0.202). The relationship between TTF and PV is also significant in a multiple regression model that contains TTF^2, TTF, age, and sex (overall p=0.280, R^2 = 0.206, TTF p=0.045; Table 4).

BrdU Cell Counts

BrdU is a thymidine analogue that incorporates into the DNA of dividing cells and, when injected, systemically marks newly generated cells. Counts of $BrdU^+$ neurons in the dentate gyrus of the hippocampus of the aging monkey brain showed a significant reduction with age[10] (p=0.008, R^2 = 0.407). When analyzed for

effects of time in cryostorage, there was no significant correlation between TTF and $BrdU^+$ neurons (p=0.293, R^2 = 0.078; Fig. 2D). There was also no relationship between TTF and $BrdU^+$ neurons in a multiple regression analysis controlling for age (TTF p=0.732, semipartial R^2 = 0.006). This study was conducted using only males, so sex was not included in the regression analysis.

DCX Cell Counts

DCX is a microtubule-associated protein found intracellularly in the somata and processes of immature neurons and neuronal precursor cells.[22] Stereological counts of DCX in the hippocampus of the aging monkey brain showed a significant decrease with age[10] (p=0.002, R^2 = 0.507). When analyzed for effects of cryostorage, there was a significant decrease in DCX cell counts with increasing TTF (p=0.033, R^2 = 0.285; Fig. 2E). However, when multiple regression was used to control for age, the relationship between TTF and DCX only approached significance (TTF p=0.086, semipartial R^2 = 0.104; age p=0.006, semipartial R^2 = 0.325; Table 4). Although the age–TTF interaction variable was not significant (p=0.193), the subtle correlation between TTF and age (r = 0.322, p=0.224) likely confounded the relationship between TTF and DCX.

ProBDNF Measures

ProBDNF is the precursor form of brain-derived neurotrophic factor, the most prevalent member of the neurotrophin family of growth factors.[23–26] ProBDNF staining was analyzed in four ways in the inferior parietal lobule (IPL) of the same cohort of aging monkeys: numbers of positively stained cell bodies and of extracellular puncta in gray matter,[27] as well as overall OD of BDNF staining in gray matter and in white matter. Two measures, proBDNF puncta and proBDNF OD in gray matter, did not correlate significantly to age or to TTF. Of the other two measures, proBDNF cell numbers in gray matter increased with age and increased with TTF, and OD in white matter did not change with age but increased with TTF. The significant increase of these two proBDNF measures relative to TTF was surprising as it is contrary to the expectation that any effect of TTF would be to reduce histochemical detection. These findings are discussed individually in the following sections.

ProBDNF Puncta Numbers Are Stable With TTF. Calibrated photomontages of the monkey IPL were acquired under matched conditions and puncta automatically identified with ImageJ. Counts of puncta demonstrated no significant change with age[27] (p=0.885, R^2 = 0.001). When analyzed for effects of time in cryostorage, there was no significant relationship between TTF and puncta number (p=0.926, R^2 < 0.001; Fig. 3B). This relationship was also not significant in a multiple regression model that included TTF, age, and sex (TTF p=0.843, semipartial R^2 = 0.001).

ProBDNF Gray Matter OD Is Stable With TTF. Because detection of puncta required thresholding, the same image montages were also analyzed for total proBDNF OD. Results showed that there was a significant age-related decrease in total proBDNF OD in the gray matter (p=0.045, R^2 = 0.112).[27] When analyzed for effects of TTF in cryostorage, there were no significant correlations between gray matter OD and TTF (p=0.959, R^2 < 0.001; Fig. 3C). This relationship was still not significant in a multiple regression model that included TTF, sex, and age (TTF p=0.848, semipartial R^2 = 0.001).

ProBDNF White Matter OD Increases With TTF. Although there was no change in proBDNF white matter OD with age (p=0.103, R^2 = 0.076), when analyzed for effects of time in cryostorage, there was a significant increase in proBDNF white matter OD with increasing TTF (p=0.048, R^2 = 0.110; Fig. 3D). This relationship was still significant in a multiple regression model that included TTF, age, and sex (TTF p=0.031, semipartial R^2 = 0.126; Table 4).

ProBDNF Cell Counts Increase With TTF. The number of proBDNF-positive cell bodies detected with ImageJ showed a surprising effect of age with cell counts increasing (p=0.011, R^2 = 0.177[27]). When analyzed for effects of time in cryostorage, proBDNF cell counts increased significantly with TTF (p=0.025, R^2 = 0.139; Fig. 3A). The relationship between TTF and proBDNF cell counts was still significant in a multiple linear regression model that included TTF, age, and sex (TTF p=0.008, semipartial R^2 = 0.165; Table 4).

Summary of ProBDNF. To summarize, four proBDNF measures in the IPL were analyzed with respect to TTF. While ProBDNF puncta and OD in the gray matter do not change with TTF, both proBDNF cell counts and OD in the white matter increase significantly with TTF. Possible explanations for this unexpected increase are presented in section “Discussion.”

Damaged Myelin Basic Protein Fluorescence Intensity

Myelin basic protein (MBP) is a component of the myelin sheath.[28] The dMBP antibody targets an

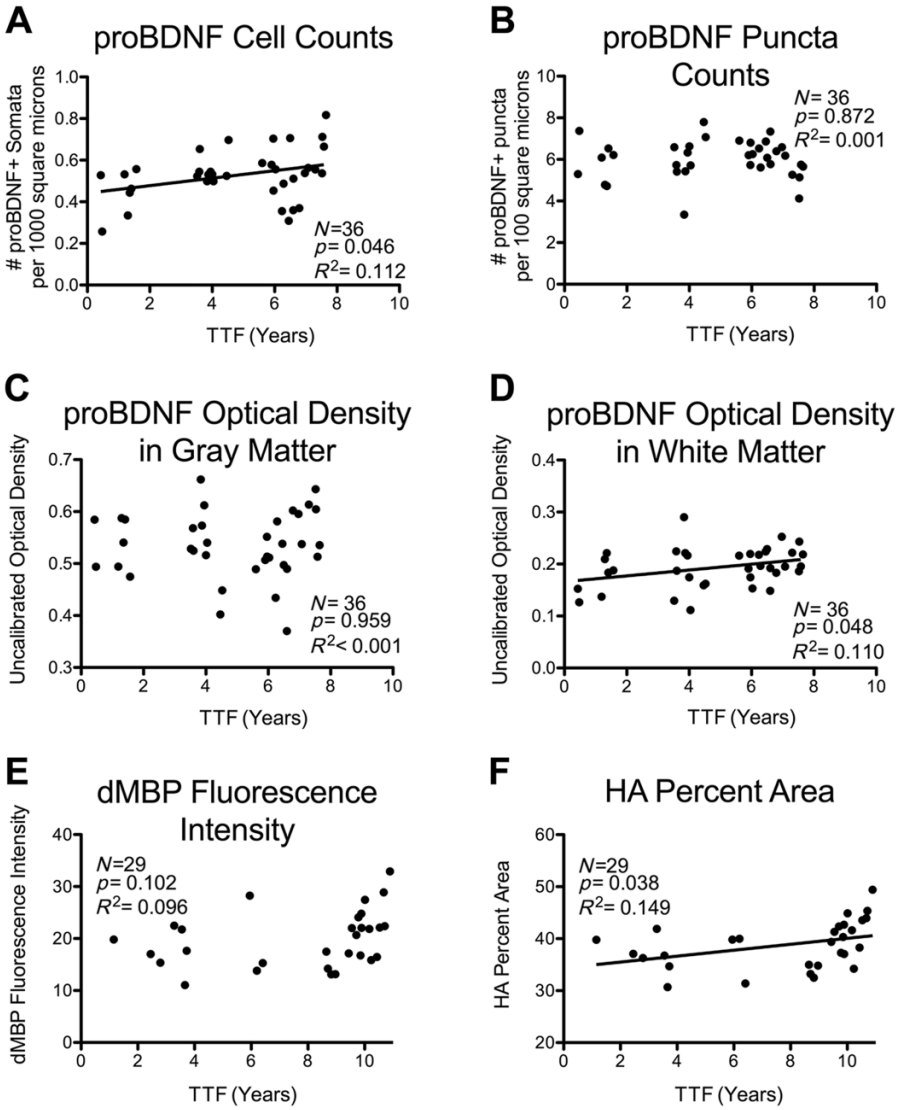

Figure 3. Simple linear correlations between TTF and measures derived from histochemical stains. TTF in years versus staining measures for the following antigens: (A) cells positive for the proBDNF, counted in IPL; (B) proBDNF^{+} puncta, counted in the IPL; (C) proBDNF uncalibrated optical density in the gray matter, (D) proBDNF uncalibrated optical density in the white matter; (E) dMBP fluorescence intensity; (F) HA percent area. Regression lines are shown for relationships that reach significance at $\alpha \leq 0.05$. Abbreviations: TTF, total time frozen; proBDNF, pro-brain-derived neurotrophic factor; IPL, inferior parietal lobule; dMBP, damaged myelin basic protein; HA, hyaluronic acid.

epitope on MBP that is concealed when MBP is intact, and is exposed when MBP is damaged or denatured,[29] serving as a marker of myelin damage.[16,17,29–31] The dMBP fluorescence intensity did not change significantly with age in the cingulum bundle in a cohort of 29 monkeys (p=0.077, R^2 = 0.111).[32] When analyzed for effects of time in cryostorage, linear regression did not show a significant relationship between TTF and dMBP (p=0.102, R^2 = 0.096; Fig. 3E).

However, because the squared term for TTF in the multiple regression model was significant (Table 4) and this indicates that the data are not entirely linear, three different non-linear quadratic models were considered: (1) a multiple regression model that included TTF^2, TTF, age, and sex (overall model p=0.012, R^2 = 0.405; Table 4); (2) a multiple regression model that included only significant predictors (same as #1 but without age, excluded due to its non-significant p value; overall model p=0.014, R^2 = 0.340); and (3) a multiple regression model that contained only TTF^2 and TTF (overall model p=0.040, R^2 = 0.220; Fig. 4A). Although these quadratic multiple regression models

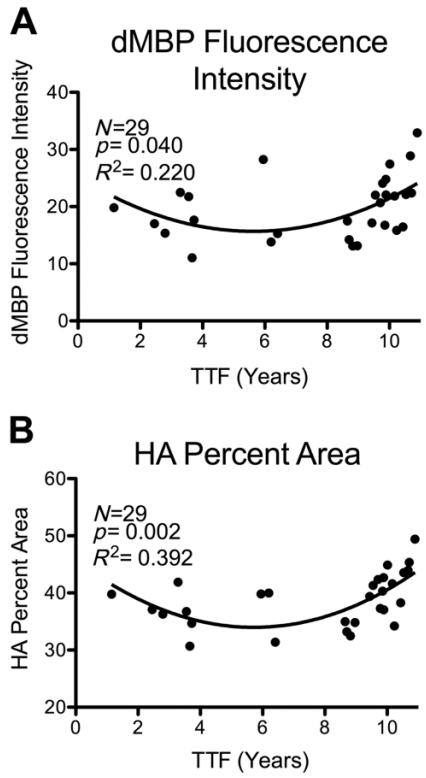

Figure 4. Quadratic models of relationships between TTF and histochemical measures. Relationships between TTF and histochemical measures in which a quadratic multiple regression model was significant. The statistics shown on each graph are for the model that includes only TTF and TTF^2. (A) dMBP fluorescence intensity; (B) HA fluorescent percent area. Compare with linear regression plots of the same datasets in Fig. 3E and F. Abbreviations: TTF, total time frozen; dMBP, damaged myelin basic protein; HA, hyaluronic acid.

more accurately describe the relationship between TTF and dMBP than a simple linear model, it is unclear why histochemical reactivity would change in a "U-shaped" quadratic pattern with cryostorage time. One possibility is that there may be an effect of storage time beyond a duration of 8 years as it appears from the scatter plot that the significance of the quadratic relationship is mostly driven by an increase in fluorescent staining, possibly background, in tissue stored longer than 8 years (Fig. 4). The superiority of the quadratic multiple regression models over the simple linear model can be seen by comparing R^2 values of each (indicative of the proportion of variance accounted for by each model): The R^2 of the best quadratic model reported above is considerably higher than that of the simple linear model (0.405 vs. 0.096). In any case, it is best to include the non-linear term when it is significant because of the increased accuracy it provides when controlling for hidden effects of TTF on the primary experimental variables of interest (such as age).

HA Percent Area

HA is an extracellular glycosaminoglycan that forms a branching scaffold structure to which other neural extracellular matrix (ECM) components attach,[33] reviewed by Sherman and Back[34] and Bignami et al.[35] The percent area of HA significantly increases in the cingulum bundle with age (p=0.025, R^2 = 0.172[32]). When analyzed for effects of cryostorage with linear regression, there was a significant increase in HA with increasing TTF (p=0.038, R^2 = 0.149; Fig. 3F). When analyzed with quadratic multiple regression models, results showed even stronger relationships between TTF and HA: (1) a quadratic multiple regression model that included TTF^2, TTF, age, and sex (overall model p=0.001, R^2 = 0.548; Table 4); (2) a quadratic multiple regression model that included only significant predictors (same as #1 but without sex, which was excluded due to its non-significant p value; overall model p=0.001, R^2 = 0.500); and (3) a quadratic multiple regression model that included only TTF^2 and TTF (p=0.002, R^2 = 0.392; Fig. 4B).

Discussion

Summary of Results

Although published studies[2,3,36] recommend approaches for long-term frozen cryostorage of sections for histochemical studies, there have been no systematic, quantitative assessments of how such storage might affect subsequent immunohistochemical processing either for specific markers or in general. In this study, we quantitatively assessed whether various quantitative measures of histochemical staining are affected by time in –80C cryostorage. Results reported here from analyses of 11 different histochemical measures indicate that most measures are stable for up to 10 years in –80C when stored as 30-µm-thick sections in buffer with 15% glycerol (after initial cryoprotection as a block with 20% glycerol). Specifically, the length of time in cryostorage at –80C had no effect on six measures: stereological cell counts for NeuN, Orexin-A, BrdU, and PV as well as image analysis estimates for $proBDNF^+$ puncta counts and OD in the gray matter. In contrast, DCX^+ cell count was the only measure to *decrease* significantly with longer frozen storage time in simple linear regression. However, multiple regression analysis suggested this could be due to a confound of the dataset in which DCX^+ cells decrease with age, and there was a correlation of TTF with age. Finally, contrary to the expectation

that extended TTF might reduce histochemical markers, four measures showed increases with TTF: ProBDNF$^+$ cell bodies in the gray matter and proBDNF OD in the white matter both increased significantly with longer TTF as did the fluorescent percent area stained by HA histochemistry. The relationship between fluorescence intensity of dMBP and TTF was not significant as assessed by simple linear regression, but a non-linear multiple regression model was significant.

It is surprising that a few relationships between TTF and measures of histochemical reactivity were significant, whereas others were not, even in the same cases processed with a single reaction (e.g., proBDNF OD in gray matter vs. white matter or proBDNF cell counts vs. puncta counts in gray matter). Particularly puzzling were the instances in which the significant effect of TTF appeared to increase staining because the expectation was that if this affected the tissue, it would reduce staining. Nevertheless, it is important to note that even in those instances where there was a significant effect of TTF as assessed by *p* value, the effect sizes as assessed in multiple regression models as R^2 were negligible—that is, accounted for very little of the variance in the data relative to the primary relationships of interest. Moreover, these small effects of TTF did not alter or confound the interpretation of the data with respect to the main variables of interest in the original studies, such as age. The cryostorage methods described here can be used for up to 10 years but should be checked with a careful multiple regression approach to detect and control for any small effects of TTF.

Commonly Used Cryoprotectant Solutions

All published cryoprotectants used to process brain tissue for IHC are either sucrose-based or glycerol-based, but there has not been a systematic comparison of IHC quality between the two means of storage. The ability of sucrose-based cryoprotectants to prevent freezing artifact is limited in large tissue blocks (e.g., ≥60 cc), where it produces inadequate and "occasionally disastrous" results.[6] Sucrose-based cryoprotection also causes tissue shrinkage, which limits the usefulness of the tissue for quantitative morphological studies.[6] For example, in one study, the average shrinkage of four monkey brain blocks cryoprotected with sucrose was 6.5%, whereas the average shrinkage of four monkey brain blocks cryoprotected with glycerol–DMSO was 0.04%.[6]

Besides the main components of buffer and either sucrose or glycerol, several additives are sometimes used. DMSO, an organosulfur compound, is recommended as an additive to the 10% and 20% glycerol cryoprotectants during infiltration of large tissue blocks[6] because it improves the rate of glycerol penetration into blocks before initial freezing. The 30% sucrose cryoprotectant recommended by de Olmos and colleagues[3] and Watson and colleagues[2] for storage of frozen blocks and free-floating tissue sections contains the additives ethylene glycol (30%) and PVP-40 (1%). Ethylene glycol is a common component of commercial antifreeze. PVP-40 is a polymer that is thought to affect the loss of water through cell membranes during the freezing of unfixed cells (such as for tissue banking, for example, see Umemura et al.[37]). A study that applied cryostorage methods for ISH histochemistry samples[4] used the de Olmos cryoprotectant described above but omitted the PVP-40.

Possible Effects of 15% Glycerol on DCX, proBDNF, and HA

It is notable that the directionality of observed relationships between frozen storage time and staining measures varies: Three markers showed significant *increases* in histochemical staining with increased frozen storage time (proBDNF$^+$ cell bodies, proBDNF OD in the white matter, and HA fluorescent percent area). Two variables appeared to have non-linear relationships with TTF, showing a decrease in staining for the first years of frozen storage and then a gradual increase as time progressed (dMBP fluorescence intensity and HA fluorescent percent area; Fig. 4). In contrast, only one measure, counts of DCX$^+$ somata, showed a significant decrease in staining with increased frozen storage time although this may be partly confounded by the decrease in DCX seen with the age of the subject, which was correlated with TTF. These different patterns have different implications and likely different mechanisms.

If cryoprotectant solutions affect antigens over time by altering histochemical reactivity, such effects would be caused by either (1) water ice altering the tissue or the antigen over time or (2) the non-water components of the cryoprotectant altering the tissue or the antigen over time.

Here, the general term "water ice" refers to water that is cooled to a solid phase either as ice crystals or in vitrified form (amorphous non-crystalline state achieved by flash freezing or the presence of a high concentration of cryoprotectant during cooling). The possibility of water ice altering tissue or its components is unlikely because if water ice was affecting the tissue, the effects of TTF should have been significant for all antigens tested. The cohorts of subjects that showed significant effects of storage time (e.g., proBDNF) and those that did not (e.g., NeuN) had a similar range of TTF values, and the cryoprotection

procedure for all subjects of all cohorts was the same. Moreover, there is no evidence that cryostorage in 15% glycerol produces observable ice crystal damage. Our cryoprotection methods[6] adequately prevent the formation of ice crystals large enough to cause "freezing artifact" damage within the tissue, as evaluated by histological assessment. Ice crystal artifact and damage are obvious in improperly processed tissue blocks. Although our cryoprotection protocols prevent formation of ice crystals during freezing, slow thawing can allow recrystallization to occur. This damage is easy to detect as shown in Fig. 5B and D. In this case (AM275), the damage occurred when the frontal lobe region of the frozen cryoprotected block was allowed to slowly thaw during cutting (inadequate replenishment of pulverized dry ice). It is notable that storage for years in the 15% glycerol does not exacerbate this (Fig. 5B vs. D) but that this kind of damage never occurs when cryoprotected sections are frozen and later thawed according to our standard protocol (Fig. 5A and C). Hence, it is unlikely that water itself would affect some antigens differently than others.

The formation of ice crystals may not directly harm tissue, but it may indicate changes in the composition of the fluid to which tissue is exposed. Effects of non-water components of cryoprotectants on tissue or its components could be due to the separation of glycerol solutions into a water fraction and a glycerol fraction during freezing, as described for the use of glycerol in tissue banking of unfixed specimens.[38] Although most of the separation likely happens in the early stage of freezing as small ice crystals fuse into larger ones (termed "recrystallization," occurring fastest at temperatures above –30C[39]), ice crystal formation may be able to continue more slowly at lower temperatures. The continual formation of ice crystals not within the tissue but within the storage vial (either formation of new ice crystals or "recrystallization"—Smaller ice crystals fusing into larger ones) can increasingly separate the glycerol-salt portion of the cryoprotectant from the growing water ice portion. Because samples for live tissue banking often remain in the glycerol-based fragment by design (to protect cells from water ice crystals), they could be exposed to environments that deviate far from physiological conditions. For instance, because buffer salts can crystallize at low temperatures and increased concentrations,[40,41] the pH of the tissue environment may change, affecting the conformation and phosphorylation state of proteins. Therefore, the extent to which a protein's structure relies on the protonation or phosphorylation state of its component amino acids may render it vulnerable to such storage environments. It is plausible that long-term freezing conditions could alter the structure of some select antigens, affecting antibody recognition or other histochemical properties and altering quantitative parameters even though qualitative features are unchanged.

Although unfixed tissue banking samples are more likely to be affected by such factors than fixed tissue, we investigated the possibility that some antigens in the present study might be more susceptible to changes based on protonation or phosphorylation state. To determine whether susceptibility to such conditions could explain the increases in histochemical reactivity observed for some measures, we conducted a structural analysis of nine of the 11 antigens (all except dMBP and HA). Data concerning protein composition and modifications were obtained from Uniprot.[42] The structural features considered included the percentage and total number of each individual amino acid within the protein, with a focus on the number and percentage of specific amino acids that can confer specific structural properties to proteins. Specifically, the factors studied included the number and proportion of charged amino acids (which would be most affected by pH changes), the number and proportion of prolines (which have a pyrrolidine ring side chain that constrains protein structure, stabilizing or destabilizing the conformation of many proteins depending on the conditions[43]), and the number and proportion of serines (a common site of phosphorylation, a posttranslational modification that affects the function of proteins often by inducing a conformational change[44]). This structural analysis did not reveal any commonalities among the antigens that appear to be affected by frozen storage or specific differences from those that are unaffected.

It is possible that the various dehydration-based effects of glycerol cryoprotectants that are observed in tissue banking protocols (e.g., conformation changes due to low pH) are not factors for fixed tissue used for histochemistry as stronger fixation appears to impede the movement of water through the tissue, as shown by slower replacement of water by cryoprotectants in tissue treated with stronger fixatives.[6] Hence, fixation may mitigate the effects of potentially dehydrating conditions during storage at –80C.

TTF and Effect Size

An important statistical consideration is whether the incongruous effects of TTF producing increases in some histochemical end points or showing non-linear relationships are strong enough to require routine consideration in histochemical studies. Analysis of the R^2 values of each statistically significant relationship (representative of the proportion of variance accounted for

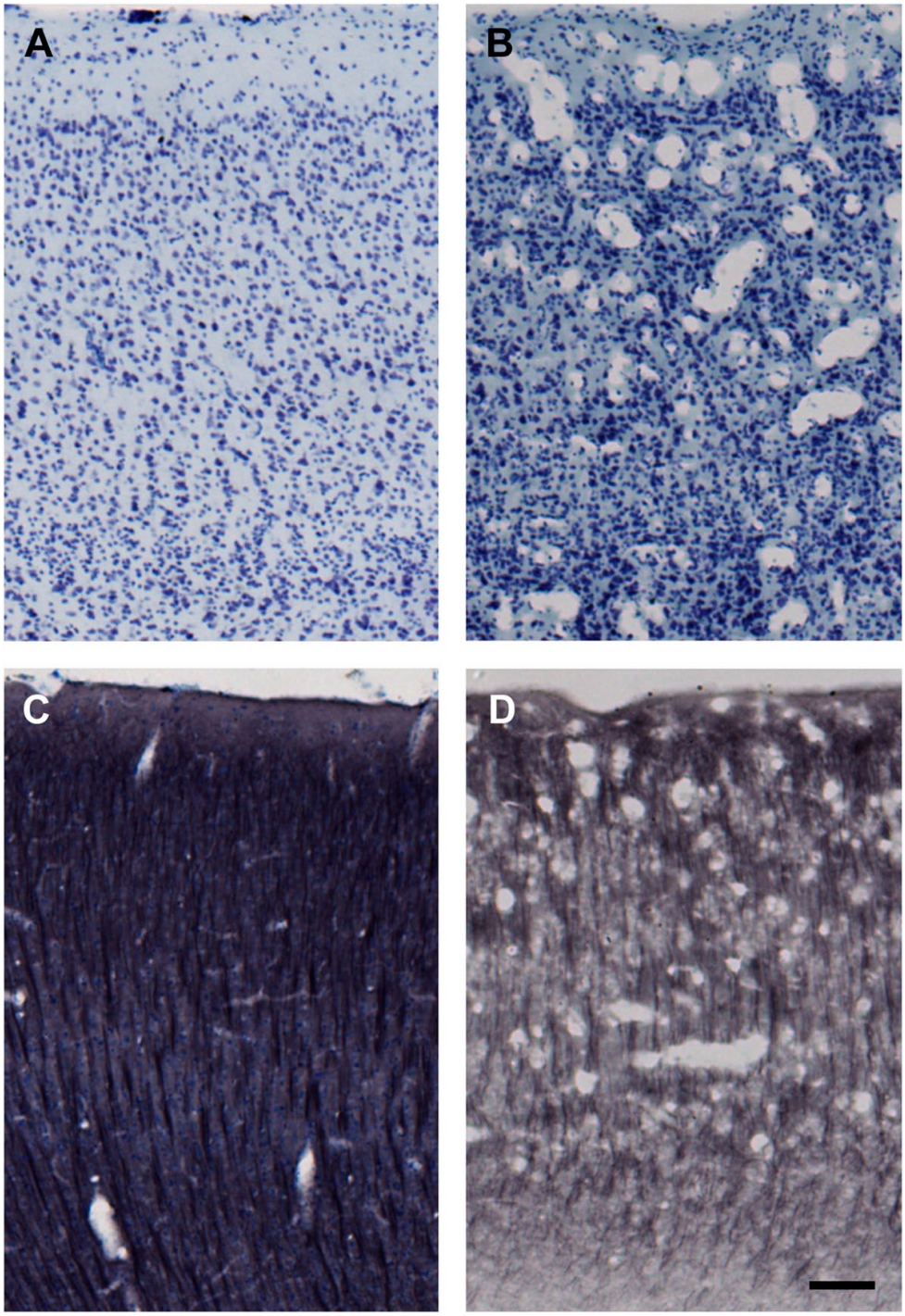

Figure 5. Freezing artifact produced before cryostorage of sections. All images are from matched locations in the ventral bank of sulcus principalis (cortical area 46). Both brains were cryoprotected using the methods reported here. (A) and (C) are from case AM177, whereas (B) and (D) are from case AM275. Sections in (A) and (B) were Nissl stained right after they were cut from the frozen block (i.e., after step #7 shown in Table 2) and without cryostorage as sections. In contrast, sections shown in (C) and (D) were immunohistochemically processed for microtubule-associated protein 2 (MAP2) with a Nissl counterstain at step #9 (Table 2) after long-term cryostorage in 15% glycerol. Freezing artifact appears as numerous vacuoles that disrupt the laminar cytoarchitecture of the cortex, as shown in case AM275 (B and D). This is likely recrystallization damage and likely occurred during cutting when the brain was inadvertently allowed to warm beyond protocol temperatures (above −30C) at the top of the block (frontal lobe) because ice crystal artifact was not present in occipital lobe sections from the bottom of the same block. Scale bar = 50 µm.

by the relationship) puts the practical impact of these relationships into context. For example, the correlation between HA percent area and TTF has an R^2 of 0.149, indicating that changes in TTF explain about 15% of the variance in the HA data. Arguably, 15% is not a high enough proportion of variance to make TTF a variable of interest. However, to err on the side of caution, multiple regression was used to control for the effects of TTF while correlating HA percent area to other measures from the original study. The aim of the original study was to determine whether there is a relationship between HA levels and myelin damage as measured by dMBP IHC, and the relationship between HA and dMBP was strong and significant ($R^2 = 0.636$ and $p<0.0001$).[32] When multiple regression was used to analyze the relationship between HA and dMBP while controlling for TTF, the relationship between HA and TTF was no longer significant. Although the simple linear regression between only HA and TTF suggests a subtle but significant relationship between the two variables (according to the p value), the strength of the relationship as measured by the effect size (according to the R^2) is so weak as to become negligible when variables with stronger relationships are considered in the analysis.

Comparison Within proBDNF Cases

The increases with TTF in two of the four proBDNF measures were unexpected as both the number of stained cell bodies in gray matter and the overall white matter OD increased with greater TTF in the same cases where the number of gray matter puncta and the overall gray matter OD were unaffected by TTF. Considering possible causes of this pattern of significance is instructive, as immunohistochemical staining of the proBDNF antigen was analyzed in three ways (cell counts, puncta counts, and OD) and in four compartments/areas (OD in the gray matter, OD in the white matter, puncta in the gray matter, and somata in the gray matter) within the same sections from the same cases. These findings present three issues for consideration. First, the subcellular compartment or location in the tissue may be an important factor affecting cryostorage vulnerability—If effects of TTF are caused by interactions between the tissue and a component of the cryoprotectant, the antigen's subcellular location may affect the degree to which it is exposed to damaging factors. Second, if freezing time does subtly affect histochemistry of vulnerable antigens, these subtle effects may be easier to detect with continuous rather than discrete measures (e.g., OD rather than cell counts)—Continuous measures can quantify subtle differences, but discrete counts can reduce degrees of staining in a cell to either "counted" or "not counted." Third, of the two proBDNF measures that showed a significant relationship with freezing time, both showed an increase in staining with increased time in frozen storage. The increase, as opposed to the expected decrease, may indicate that some aspect(s) of cryostorage interact with histochemical processing in ways that have not been considered, beyond simple tissue degradation and damage. Furthermore, it raises the possibility that potentially confounding effects of long-term cryostorage are commonly overlooked, because TTF would not be a factor suspected in an unexplained increase in staining.

Recommended Methods for Cryoprotection and Cryostorage for Batch-Processing

As previously described[6] and summarized above in section "Materials and Methods," fixed tissue blocks of any size up to 150 cc are cryoprotected by infiltration with glycerol cryoprotectant (10% glycerol and 2% DMSO in buffer at 4C for 1–3 days, and then with 20% glycerol and 2% DMSO at 4C for at least 4 days). Once equilibrated, the brain is flash frozen in –75C isopentane to minimize ice crystal formation. After an hour in –75C isopentane, the block is wrapped in foil, placed in a sealed plastic jar, and stored at –80C until cut on a freezing microtome into frozen sections. As the block is cut onto a room temperature knife (while the block is kept at –60C with dry ice), the sections thaw rapidly onto the blade avoiding recrystallization artifact. It is worth noting that frozen tissue blocks cryoprotected with glycerol cannot be cut on a cryostat at –20C to –40C because the sections are not completely frozen and so do not come off onto the knife as a wafer nor can they completely thaw. The result is that they stick to the cryostat blade. On the freezing microtome, the sections that thaw onto the blade are removed with a moist paintbrush and placed into vials with 15% glycerol in buffer. These vials are stored at 4C overnight to allow the sections to equilibrate, and are then placed into a –80C freezer for storage until needed for histochemistry.

During immunohistochemical processing of the tissue sections, it is important to process all sections in the same batch of reagents, for the same amounts of time—a technique referred to as "batch-processing." This is crucial to minimize variations in staining quality between subjects or sections due to slight differences in reagent strength or incubation timing.

Possible Pitfalls and Limitations

The present study demonstrates that the recommended methods described above should preserve brain tissue quality for quantitative histochemistry for

most molecules up to at least 10 years. However, when using this approach, it is advisable to evaluate IHC quality as follows: Perform quantitative histochemistry as described above with batch-processing of tissue samples that have been in frozen storage the longest, alongside tissue that has recently been processed and frozen. Quantify the label and then perform multiple regression analysis on the resulting data to determine whether time frozen affects staining when controlling for other significant factors of interest, such as age, drug treatment, sex, and so on. All standard assumptions of multiple regression should be tested, including assessing the linearity of data and checking for interaction effects. If a significant association does exist between time frozen and the quantified staining measure, use of multiple regression will control for the effects of freezing time in the data. Long-term frozen storage of tissue sections using the methods described here generally preserves histochemical reactivity for frozen sections of fixed brain tissue. For the subset of the labels that did show a subtle relationship with frozen storage time, the effect size is likely to be negligible when analyzed in conjunction with the main variables of interest from their original studies. Nevertheless, it is advisable to include TTF as a variable in a multiple regression analysis to ensure that it has not confounded the main effect. Even if a histochemical label does appear to be affected by frozen storage time, and multiple regression demonstrates that this actually confounds the results for that marker, the present results demonstrate that the same tissue might still be useful for investigations of other antigens as effects are antigen specific.

Acknowledgment

We thank Karen Slater, Penny Shultz, Alana Carmichael, and Samantha Calderazzo for invaluable technical assistance.

Competing Interests

The author(s) declared no potential conflicts of interest with respect to the research, authorship, and/or publication of this article.

Author Contributions

Histochemistry data were acquired and provided by the following authors: neuronal nuclei and parvalbumin data from ELG, orexin-A from DER, all pro-brain-derived neurotrophic factor from AAR, doublecortin and bromodeoxyuridine from LBN and NCH, and hyaluronic acid and damaged myelin basic protein from LIE. DLR and LIE designed the study and drafted the manuscript. FM and ACA contributed to study design and implementation. AAR provided the comparative analysis of antigen amino acid composition. HJC and RJK provided consultation on statistical procedures and interpretation. All authors have read and approved the final manuscript.

Funding

The author(s) disclosed receipt of the following financial support for the research, authorship, and/or publication of this article: Research support from National Institutes of Health (NIH) grants P01-AG000001, R01-AG043640, and R01-AG042512; National Institute of General Medical Sciences (NIGMS) Training Grant T32GM008541, and National Science Foundation (NSF) grants PHY-0855161, PHY-1505000, and PHY-1444389.

Literature Cited

1. Giannaris EL, Rosene DL. A stereological study of the numbers of neurons and glia in the primary visual cortex across the lifespan of male and female rhesus monkeys. J Comp Neurol. 2012;520:3492–508.
2. Watson RE, Wiegland SJ, Clough RW, Hoffman GE. Use of cryoprotectant to maintain long-term peptide immunoreactivity and tissue morphology. Peptides. 1986;7:155–9.
3. de Olmos JS, Hardy H, Heimer L. The afferent connections of the main and the accessory olfactory bulb formations in the rat: an experimental HRP study. J Comp Neurol. 1978;181:213–44.
4. Lu W, Haber SN. In situ hybridization histochemistry: a new method for processing material stored for several years. Brain Res. 1992;578:155–60.
5. Milner TA, Waters EM, Robinson DC, Pierce JP. Degenerating processesidentified by electron microscopic immunocytochemical methods. In: Manfredi G, Kawamata H, editors. Neurodegeneration: methods and protocolsmethods in molecular biology. vol. 793. New York: Springer; 2011. p. 23–59. doi:10.1007/978-1-61779-328-8_3.
6. Rosene DL, Roy NJ, Davis BJ. A cryoprotection method that facilitates cutting frozen sections of whole monkey brains for histological and histochemical processing without freezing artifact. J Histochem Cytochem. 1986;34:1301–15.
7. Tigges J, Gordon TP, McClure HM, Hall EC, Peters A. Survival rate and life span of rhesus monkeys at the Yerkes Regional Primate Research Center. Am J Primatol. 1988;15(3):263–73.
8. Peters A, Rosene DL, Moss MB, Kemper TL, Abraham CR, Tigges J, Albert MS. Neurobiological bases of age-related cognitive decline in the rhesus monkey. J Neuropathol Exp Neurol. 1996;55:861–74.
9. Institute of Laboratory Animal Resources Commission of Life Sciences National Research Council. Guide for the care and use of laboratory animals. 8th ed. Washington, DC: National Academies Press; 2011.
10. Ngwenya LB, Heyworth NC, Shwe Y, Moore TL, Rosene DL. Age-related changes in dentate gyrus cell numbers, neurogenesis, and associations with cognitive impairments in the rhesus monkey. Front Syst Neurosci. 2015;9:102.

11. Hoffman GE, Le WW, Sita LV. The importance of titrating antibodies for immunocytochemical methods. Curr Protoc Neurosci. 2008;45:2.12.1–2.12.26.
12. Shi SR, Cote RJ, Taylor CR. Antigen retrieval immunohistochemistry: past, present, and future. J Histochem Cytochem. 1997;45(3):327–43.
13. Ripellino JA, Klinger MM, Margolis RU, Margolis RK. The hyaluronic acid binding region as a specific probe for the localization of hyaluronic acid in tissue sections. Application to chick embryo and rat brain. J Histochem Cytochem. 1985;33:1060–6.
14. West MJ, Slomianka L, Gundersen HJ. Unbiased stereological estimation of the total number of neurons in the subdivisions of the rat hippocampus using the optical fractionator. Anat Rec. 1991;231:482–97.
15. Schneider CA, Rasband WS, Eliceiri KW. NIH Image to ImageJ: 25 years of image analysis. Nat Methods. 2012;9(7):671–5.
16. Yamamoto Y, Ihara M, Tham C, Low RW, Slade JY, Moss T, Oakley AE, Polvikoski T, Kalaria RN. Neuropathological correlates of temporal pole white matter hyperintensities in CADASIL. Stroke. 2009;40(6):2004–11.
17. Ihara M, Polvikoski TM, Hall R, Slade JY, Perry RH, Oakley AE, Englund E, O'Brien JT, Ince PG, Kalaria RN. Quantification of myelin loss in frontal lobe white matter in vascular dementia, Alzheimer's disease, and dementia with Lewy bodies. Acta Neuropathol. 2010;119:579–89.
18. Mullen RJ, Buck CR, Smith AM. NeuN, a neuronal specific nuclear protein in vertebrates. Development. 1992;116(1):201–11.
19. Kim KK, Adelstein RS, Kawamoto S. Identification of neuronal nuclei (NeuN) as Fox-3, a new member of the Fox-1 gene family of splicing factors. J Biol Chem. 2009;284(45):31052–61.
20. de Lecea L, Kilduff TS, Peyron C, Gao XB, Foye PE, Danielson PE, Fukuhara C, Battenberg ELF, Gautvik VT, Bartlett FS 2nd, Frankel WN, van den Pol AN, Bloom FE, Gautvik KM, Sutcliffe JG. The hypocretins: hypothalamus-specific peptides with neuroexcitatory activity. Proc Natl Acad Sci U S A. 1998;95:322–7.
21. Andressen C, Blümcke I, Celio MR. Calcium-binding proteins: selective markers of nerve cells. Cell Tissue Res. 1993;271:181–208.
22. Brown JP, Couillard-Despres S, Cooper-Kuhn CM, Winkler J, Aigner L, Kuhn HG. Transient expression of doublecortin during adult neurogenesis. J Comp Neurol. 2003;467(1):1–10.
23. Mufson EJ, Kroin JS, Sendera TJ, Sobreviela T. Distribution and retrograde transport of trophic factors in the central nervous system: functional implications for the treatment of neurodegenerative diseases. Prog Neurobiol. 1999;57:451–84.
24. Poo MM. Neurotrophins as synaptic modulators. Nat Rev Neurosci. 2001;2:24–32.
25. Lu B, Pang PT, Woo NH. The yin and yang of neurotrophin action. Nat Rev Neurosci. 2005;6:603–14.
26. Barker PA. Whither proBDNF? Nat Neurosci. 2009;12:105–6.
27. Robinson AA, Rosene DL. Quantification of proBDNF immunoreactivity in the inferior parietal lobule of the aging rhesus monkey. Program No. 243.06. 2012 Neuroscience Meeting Planner. New Orleans: Society for Neuroscience. Online; 2012.
28. Harauz G, Ladizhansky V, Boggs JM. Structural polymorphism and multifunctionality of myelin basic protein. Biochemistry. 2009;48:8094–104.
29. Matsuo A, Lee GC, Terai K, Takami K, Hickey WF, McGeer EG, McGeer PL. Unmasking of an unusual myelin basic protein epitope during the process of myelin degeneration in humans. Am J Pathol. 1997;150(4):1253–66.
30. Matsuo A, Akiguchi I, Lee GC, McGeer EG, McGeer PL, Kimura J. Myelin degeneration in multiple system atrophy detected by unique antibodies. Am J Pathol. 1998;153(3):735–44.
31. Wu H, Wu T, Mingchang L, Wang J. Efficacy of the lipid-soluble iron chelator 2,2′-dipyridyl against hemorrhagic brain injury. Neurobiol Dis. 2012;45(1):388–94.
32. Estrada LI. Histochemical markers of myelin damage and impaired remyelination in the aging rhesus monkey brain: relationship to cognitive performance [dissertation]. Boston: Boston University; 2016. ProQuest Dissertations Publishing.
33. Scott JE, Cummings C, Brass A, Chen Y. Secondary and tertiary structures of hyaluronan in aqueous solution, investigated by rotary shadowing-electron microscopy and computer simulation. Hyaluronan is a very efficient network-forming polymer. Biochem J. 1991;274:699–705.
34. Sherman LS, Back SA. A "GAG" reflex prevents repair of the damaged CNS. Trends Neurosci. 2008;31(1):44–52.
35. Bignami A, Hosley M, Dahl D. Hyaluronic acid and hyaluronic acid-binding proteins in brain extracellular matrix. Anat Embryol. 1993;188:419–33.
36. Hoffman GE, Le WW. Just cool it! Cryoprotectant antifreeze in immunocytochemistry and in situ hybridization. Peptides. 2004;25:425–31.
37. Umemura E, Yamada Y, Nakamura S, Ito K, Hara K, Ueda M. Viable cryopreserving tissue-engineered cell-biomaterial for cell banking therapy in an effective cryoprotectant. Tissue Eng Part C. 2011;17(8):799–807. doi:10.1089/ten.tec.2011.0003.
38. Morris GJ, Goodrich M, Acton E, Fonseca F. The high viscosity encountered during freezing in glycerol solutions: effects on cryopreservation. Cryobiology. 2006;52(3):323–34.
39. Asahina E, Shimada K, Hisada Y. A stable state of frozen protoplasm with invisible intracellular ice crystals obtained by rapid cooling. Exp Cell Res. 1970;59(3):349–58.
40. Pikal-Cleland KA, Rodriguez-Hornedo N, Amidon GL, Carpenter JF. Protein denaturation during freezing and thawing in phosphate buffer systems: monomeric and

tetrameric beta-galactosidase. Arch Biochem Biophys. 2000;384(2):398–406.
41. Murase N, Franks F. Salt precipitation during the freeze-concentration of phosphate buffer solutions. Biophys Chem. 1989;34:293–300.
42. Leinonen R, Garcia Diez F, Binns D, Fleischmann W, Rodrigo Lopez R, Apweiler R. UniProt archive. Bioinformatics. 2004;20(17):3236–37.
43. Prajapati RS, Das M, Sreeramulu S, Sirajuddin M, Srinivasan S, Krishnamurthy V, Ranjani R, Ramakrishnnan C, Varadarajan R. Thermodynamic effects of proline introduction on protein stability. Proteins. 2007;66:480–91.
44. Kim SY, Jung Y, Hwang GS, Han H, Cho M. Phosphorylation alters backbone conformational preferences of serine and threonine peptides. Proteins. 2011;79:3155–65.